Molding of Syndiotactic Polystyrene Under Its Melting Temperature

LUIGI ABBONDANZA, FABIO GARBASSI, ANTONIO GENNARO, GIORGIO GIANNOTTA, GIANLUIGI MARRA, RICCARDO PO′, FRANCESCO TOSCANI

EniChem S.p.A., Centro Ricerche Novara, Istituto Guido Donegani, Via Fauser 4, 28100 Novara, Italy

Received 27 February 2000; accepted 3 June 2000

ABSTRACT: Syndiotactic polystyrene (SPS), a thermoplastic polymer that exhibits a high T_m in some crystalline forms, can be conveniently processed by a cold-compaction technique. Processing temperatures in the range of 150–210°C, well below the T_m, gives rise to physicomechanical properties comparable and even better than those obtained by thermal compression or injection molding. The optimum treatment temperature seems to fall around 175°C. X-ray diffraction analysis, thermal analysis, and density measurements suggest that such behavior is connected to phase transitions of SPS and favored by the presence of styrene included in the crystalline fraction. © 2001 John Wiley & Sons, Inc. J Appl Polym Sci 80: 377–383, 2001

Key words: syndiotactic polystyrene; cold compression molding; phase transitions; crystallinity; mechanical properties

INTRODUCTION

Conventional processing technologies such as extrusion, injection molding, and calendering are difficult to apply to some polymeric materials, showing a very high melt viscosity, like ultra-high-molecular-weight polyethylene (UHMWPE)[1,2] and poly(tetrafluoroethylene) (PTFE).[2] In such cases it has been necessary to find a specific manufacturing process. For instance, in the case of UHMWPE a process consisting of two distinct stages has been developed.[3] In the first stage the powder material is compacted under high hydrostatic pressure, followed by sintering at high temperature, when particles coalesce and voids are eliminated. The suitable sintering temperature was found to be a temperature higher than the melting temperature (T_m) of the polymer. Good powder aggregation can be obtained only when pressure produces a molecular rearrangement at the particles interfaces. This behavior was preferentially observed in semicrystalline polymers having secondary transitions between the glass-transition temperature (T_g) and T_m.[4]

Syndiotactic polystyrene (SPS), synthesized by Ishihara by means of a catalytic system formed by a Ti organometallic compound and methylaluminoxane,[5] exhibits a set of interesting properties, such as very high T_m, excellent resistance to chemicals, water and steam, low dielectric constant, high elasticity modulus and low permeability to gases.[6] Connected to the high value of SPS T_m is the necessity to set up suitable and energy saving processing technologies.

SPS exhibits a rather complex polymorphism. At least four crystalline forms have been observed and their molecular structures determined.[7] The α-form, which can be obtained by compression

Correspondence to: F. Garbassi (fabio.garbassi@enichem.it).

Journal of Applied Polymer Science, Vol. 80, 377–383 (2001)

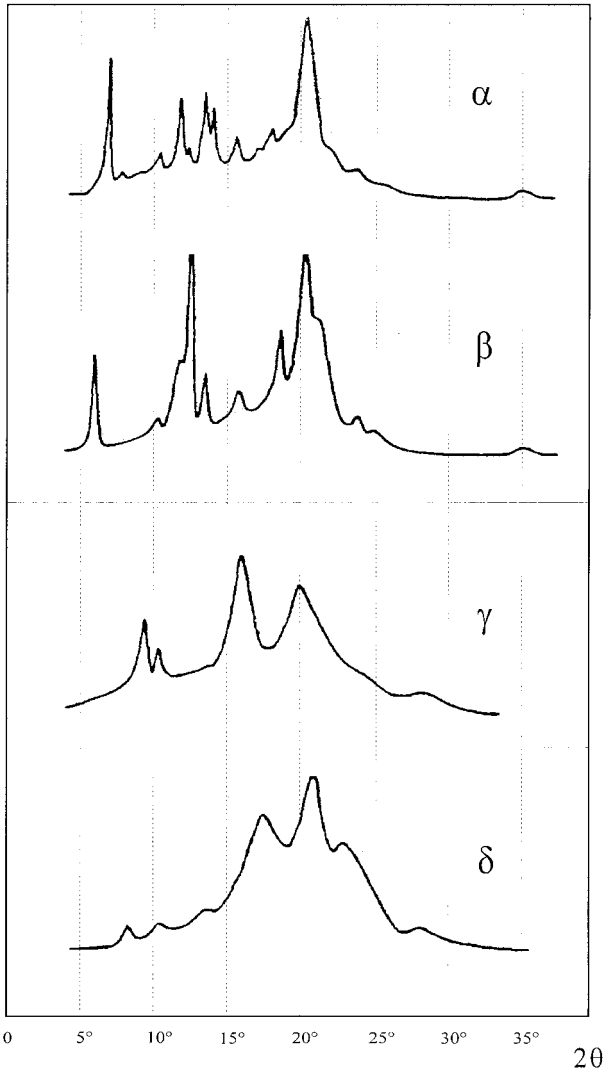

Figure 1 X-ray diffraction patterns of crystalline forms of SPS (with permission from Guerra et al.[7]).

molding, and the β-form, obtained by solvent casting at high temperature or from melt at low cooling rates, are characterized by the presence of a zigzag planar conformation of chains and an identity period of 0.51 nm.[8] Swelling of α-form samples in different solvents, followed by evaporation of solvent excess, produces the γ- and δ-forms, characterized by an identity period of 0.77 nm.[9] Both forms include solvent or unreacted monomer (i.e., styrene) molecules in the crystalline structure. Each of these crystalline forms is associated with a particular X-ray diffraction pattern, as shown in Figure 1. The conditions for transition from one form to another have been determined,[10] as reported in Figure 2.

Starting from this background, a study was conducted with the aim of finding a convenient molding method of SPS.

EXPERIMENTAL

Materials

Syndiotactic polystyrene was prepared in the laboratory according to a previously reported procedure.[11] The reaction product was killed in methanol and NaOH, then extracted with methyl ethyl ketone for 8 h in order to eliminate the atactic fraction. Finally, it was dried in N_2 at 80°C for 8 h and at 150°C for 4 h. This produced a crystalline powder with a molecular weight (MW) of about 300,000 Da, as measured by gel permeation chromatography (GPC), and a T_g of 100°C and T_m of 274°C, according to differential scanning calorimetry (DSC). The XRD diagram indicated the presence of a γ crystalline form, known to be a clathrate phase.[9] In fact, the material contained in the structure was styrene, estimated to be below 2% by weight.

For the sake of comparison, the following materials were also considered:

- fiber-grade poly(ethylene terephthalate) (PET) from Montefibre, Acerra, Italy, with a MW of 32000 Da; and

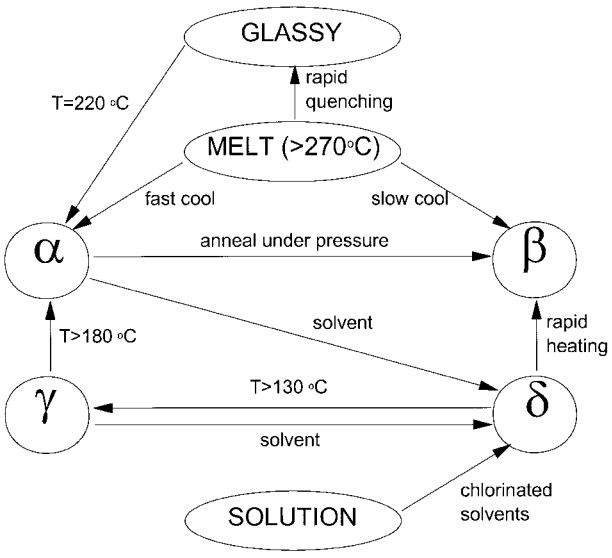

Figure 2 Simplified representation of crystalline and state transitions in SPS.

Table I Thermal Properties of Polymers and Temperatures at Which Experiments Were Carried Out

Polymer	T_g (°C)	T_m (°C)	Cold Compaction Range (°C)	Compression Molding (°C)
SPS	100	274	120–210	290
PET	75	260	170–230	270
LLDPE	−30	118	60–100	200

- low-density linear polyethylene (LLDPE) from Polimeri Europa, Flexirene CL10, with an MFI of 2.5 g/10 min at 190°C (weight 2.16 kg).

For all these materials, powder fractions with an average diameter of 50 μm were used for molding experiments. PET and LLDPE powders were obtained by cryogrinding, followed by heating under vacuum at 60°C for 8 h.

Physicochemical Characterization of Polymers

Molecular weights of SPS were measured by a Waters 150C GPC instrument operating at 135°C in 1,2,4-trichlorobenzene and using atactic polystyrene as a standard. DSC runs were carried out with a PerkinElmer DSC-7 calorimeter, at a heating temperature rate of 20°C/min. During cooling at a rate of 10°C/min, crystallization temperatures (T_{cc}) were measured. The occurrence of different crystalline phases of SPS was observed by means of X-ray diffraction experiments in a Siemens D500 θ/θ diffractometer operating with CuKα radiation and reflection geometry. A solid-state NaI scintillation detector was also used. Crystallinity was measured by Ruland's method, with the assumption that that obtained by quenching the SPS melt was representative of the amorphous spectrum. The following peak intensities were taken into account when the fractions of the crystalline forms were measured: 6.73° and 11.65° for the α-form, 6.11° and 12.3° for the β-form, and 9.25° for the γ-form (Fig. 1).

Molding

Cold compaction molding was carried out by means of a Moore hydraulic press equipped with thermal regulation (F_{max} 30 t, T_{max} 400°C). A piston die having a diameter of 80 mm was used to form 3.2-mm-thick disks. A pressure of 50 MPa was exerted on polymer powders for 3 min in the temperature ranges reported in Table I, which also shows the respective T_g and T_m values.

A second set of specimens from the same powders was prepared by melt pressing at temperatures higher than T_m for 10 min under a pressure of 5 MPa, using a cavity of 100 × 100 × 3.2 mm between two stainless-steel sheets (2 mm thick) covered with aluminum foil.

Physicomechanical Characterization of Molded Specimens

Density measurements of polymer specimens after molding were done with an analytical balance. Shear strengths were measured with an Instron 4502 universal testing machine on dumbbells according to ASTM D638 at the rate of 1.2 mm/min. The impact strength (Izod method) was measured according to ASTM D256 on notched rods, using a 2.7 J hammer.

RESULTS AND DISCUSSION

X-ray diffractograms of SPS compacted at various temperatures are reported in Figure 3. For the sake of comparison, the XRD spectrum of SPS thermally treated at 180°C is also shown. In the latter case, only the characteristic peaks of the γ-form are visible (Fig. 1), while after cold com-

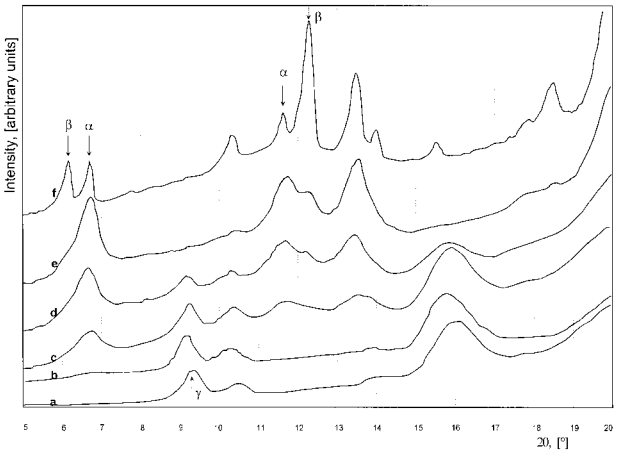

Figure 3 X-ray diffraction patterns of SPS after processing treatments: (a) thermal treatment at 180°C; (b) cold compaction at 160°C; (c) cold compaction at 175°C; (d) cold compaction at 180°C; (e) cold compaction at 210°C; (f) compression molding at 290°C.

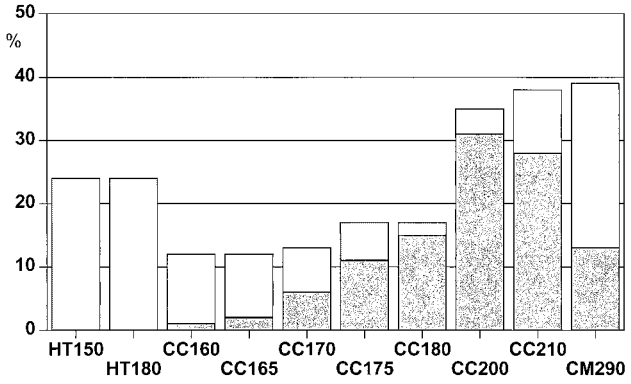

Figure 4 Crystallinity and phase distribution of SPS as a function of processing treatment (light gray: γ-phase; dark gray: α-phase; white: β-phase; HT: heat treatment; CC: cold compaction; CM: compression molding).

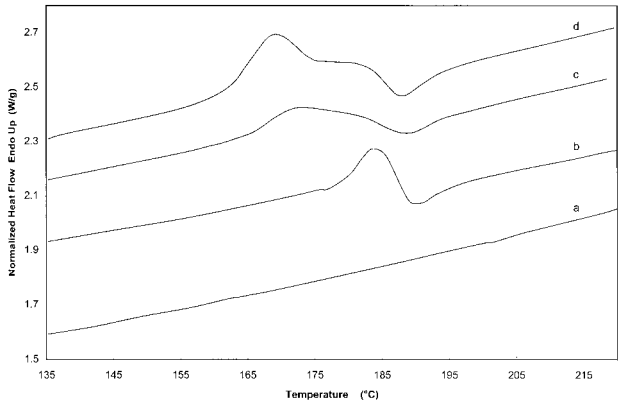

Figure 5 DSC diagrams of SPS: (a) compression molding at 290°C; (b) cold compaction at 165°C; (c) cold compaction at 180°C; (d) as prepared.

pacting at 160°C, a diffraction peak characteristic of the α-form begins to be visible at a 2θ value of 11.65°, becoming very evident after treatments at higher temperatures. By further increasing the treatment temperature, the α-form fraction increases, and the γ-form fraction decreases, until the latter disappears, at around 200°C. At a compacting temperature of 180°C, a diffraction peak at $2\theta = 12.3°$ appears, also due to the occurrence of the β-form. The fraction of such a phase increases with the treatment temperature, in agreement with the literature.[12] In addition, the total crystalline fraction increases with temperature, as shown in Figure 4, where the relative amount of each phase is indicated by a bar. Conventional compression molding of SPS at 290°C gives rise to a total crystallinity comparable to that measured on compacted samples and the presence of both α- and β-forms. Because of the overlapping of the diffraction peaks of the two crystalline forms, a relatively large uncertainty between such phases was considered.

Some representative portions of DSC diagrams of SPS cold-compacted at various temperatures are reported in Figure 5. Apart from T_g transitions and T_m peaks, which are not shown, two relevant structures are present, an endothermic peak in the range 155–190°C and an exothermic peak in the range 190–220°C. The first one is attributable to the fusion of γ-form crystallites,[7,13] while the second is due to crystallization as a phase of the amorphous fraction.[7,13] The experimental diagram is the result of the sum of enthalpic variations in the two processes. Adopting the same scanning rate for all samples, the transformation time is constant; thus it is possible to consider the surface under the endothermic peak as directly proportional to the residual crystalline phase in the powder, that is, to the γ-form. The diagram of enthalpic variations as a function of compaction temperature (Fig. 6) confirms that the amount of such a crystalline form decreases rapidly in the 160–190°C range, up to a complete disappearance. From comparing the fusion enthalpy of SPS crystal, that is, 53 J/g,[14] with those measured, it can be concluded that all samples have a total crystallinity in the range 56–62%, much higher than that drawn from XRD data. This conclusion was confirmed by the high T_g values, indicating an amorphous phase tightly linked to crystallites, and consequently present in

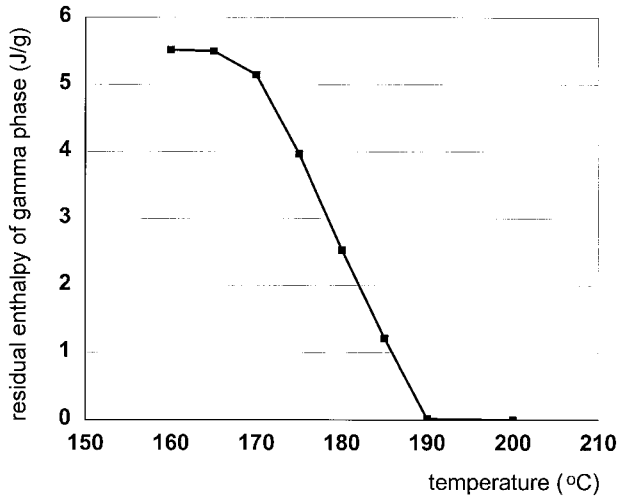

Figure 6 Enthalpy of fusion (ΔH_m) of γ-phase after cold compaction at various temperatures.

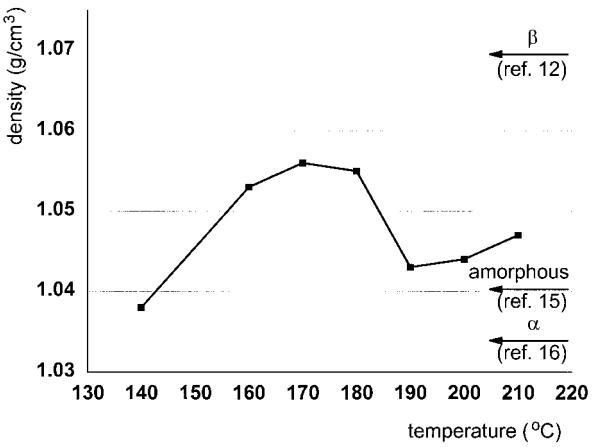

Figure 7 SPS density as a function of cold-compaction temperature.

a limited amount, and by the low values assumed by Δc_p (T_g), which is an extensive variable depending on the amorphous phase. Assuming a value of 0.28 (J °C^{-1} g^{-1})[14] for amorphous SPS, the amount of such a phase in our samples is not more than 33%. The discrepancy between the XRD and DSC results can be explained by assuming the γ-phase does not form extended crystalline regions but is present in small domains constituting paracrystalline regions.

Figure 7 shows the behavior of density as a function of compaction temperature. The behavior is clearly not linear and first shows an increase, reaching a maximum near 170°C, then a decrease, and finally an increase again. Some density values in the literature are indicated in the same graph. The solvated δ-form has a low density,[9] while the empty δ-form density is higher.[15] A further density increase was found for the γ-form,[14] while in the α-form a density decrease occurs.[16] Finally, the β-form again has a higher density.[12] According to the transformation scheme reported in Figure 2, the order of citation of these crystalline forms corresponds to the increase in temperature necessary to obtain them. Because of this, it is likely that the density behavior reported in Figure 7 is connected to the transformations that occurred, as shown by the XRD.

The behavior of several physicomechanical properties—elastic modulus, tensile strength, elongation at break, as well as impact strength—as functions of compaction temperature are presented in Figure 8. In the temperature range considered, the modulus shows a clear tendency to decrease, even if some scattering of data occurs. It shows values higher than the reference at lower temperatures, and lower than the reference at higher temperatures. Tensile strength and elongation at break values show a stepped increment in the same interval, centered in both cases at a temperature of around 175°C,

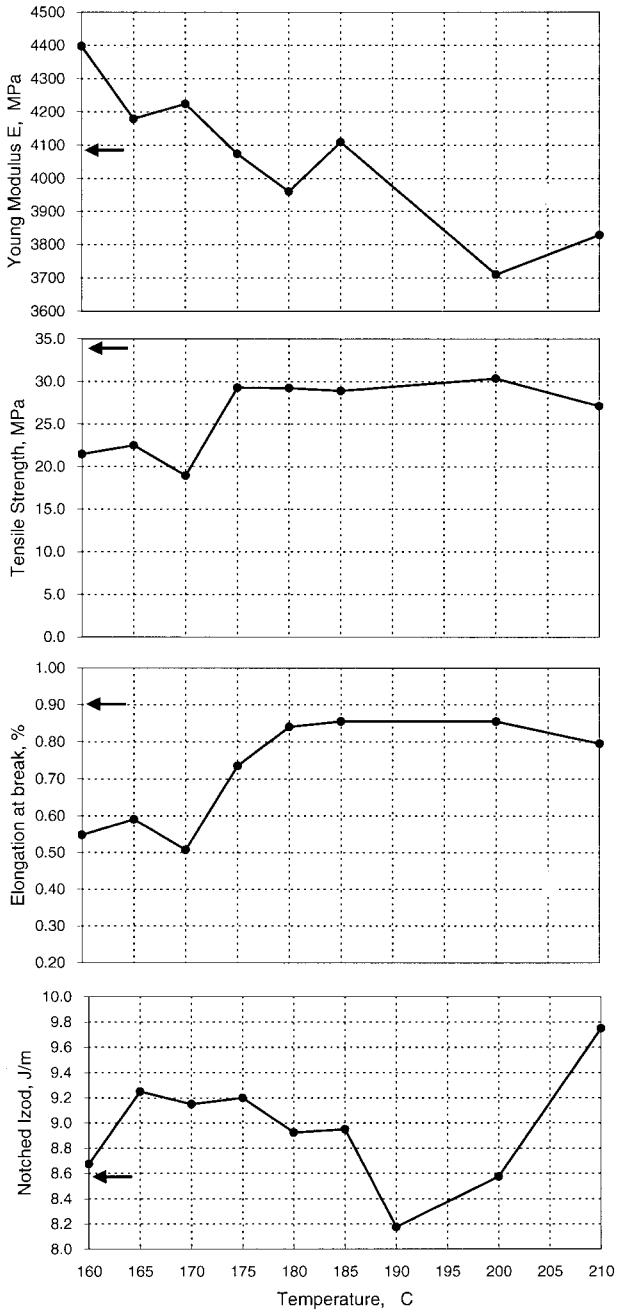

Figure 8 Physicomechanical properties of SPS as a function of cold compaction temperature. Arrows indicate the corresponding values obtained by compression molding.

Table II Physicomechanical Properties of SPS Processed by Conventional Techniques

Processing Technique	Temperature (°C)	E (Mpa)	σ_B (Mpa)	ε_B (%)	Impact Strength (Izod, J/m)
Compression molding	290	4090	34	0.9	8.6
Injection molding	290	4150	59	1.8	13.0

and reaching values comparable to the reference. The impact strength, beginning from a value comparable to that of the reference, exhibits a temperature range of higher values, then a decrease, and finally a huge increase. It is worth nothing that the most relevant changes in physicomechanical properties occur in correspondence to the density maximum, which, in turn, falls during the structural transformation from the γ- to the α-form. This is reminiscent of the behavior of polymers such as poly(oxymethylene), poly(ethylene oxide), and polyvinyl fluoride that exhibit a secondary crystalline relaxation below T_m when submitted to solid-state extrusion.[4] Only such materials were found suitable for this type of processing. However, it should be noted that, apart from a different technique, the interval between the processing temperature and T_m in the present case is as high as 90°C, while in solid-state extrusion it is necessary to operate at only 10°C under melting. Physicomechanical properties of SPS processed by means of compression molding or injection molding are reported in Table II. From comparing such data with those reported in Figure 8, it appears that cold compaction gives rise to mechanical properties not far from those obtained by injection molding and even better than those obtained by compression molding. Another interesting advantage of cold compaction is the ability to obtain results at a lower temperature; consequently, the material is less damaged from thermal degradation, requires a lower amount of thermal stabilizers for processing, and allows some energy saving. Finally, thick walls do not constitute a technological limit as they do in injection molding.

In order to check if the above results are specific to SPS or to the cold compaction technique, two other materials were chosen for the experiments in order to compare results. PET was chosen because it is a semicrystalline polymer with a T_g and T_m (75°C and 260°C, respectively) not far from those of SPS. LLDPE was chosen as a semicrystalline polymer with lower T_g and T_m values (−20°C and 130°C, respectively). Incidentally, LLPE is one of the polymers that exhibits crystalline relaxation (near 80°C).[4]

Compaction experiments of PET were carried out at 170°C and 200°C. Results of physicomechanical characterization are reported in Table III and compared with those obtained on the same material in a conventional way (compression molding at 270°C). Both deformation yield and impact strength of cold-compacted powders appear much lower than the same properties in samples prepared by thermal compression. In the case of LLDPE, the comparison is even worse because it turned out to be impossible to prepare specimens with sufficient cohesion. Treatment temperatures up to 100°C were used in the experiment.

CONCLUSIONS

By cold-compaction treatment of SPS powders at a temperature well below T_m, processing of this polymer was found possible and its physicome-

Table III Physicomechanical Properties of PET after Processing

Processing Technique	Temperature (°C)	E (Mpa)	σ_B (Mpa)	ε_B (%)	Impact Strength (Izod, J/m)
Cold compaction	170	3132	9.9	0.37	10.5
Cold compaction	200	3080	8.7	0.32	12.0
Compression molding	270	2256	27.5	300	47.4

chanical properties proved to be comparable to those of the same material submitted to compression molding. The optimal treatment temperature corresponded to a density maximum of the material and to a transition phase from the γ- to the α-form. Parallel experiments on PET and LLDPE suggest that the behavior of SPS is a peculiarity of such a polymer, likely connected to its polymorphic nature. As to possible applications, the proposed treatment could be relevant in an efficient and energy-saving processing of syndiotactic polystyrene.

REFERENCES

1. Truss, R. W.; Han, K. R.; Wallace, J .F.; Geil, P. H. Polym Eng Sci 1980, 20, 747.
2. Jog, J. P. Adv Polymer Technol 1993, 12, 281.
3. Han, K. R.; Wallace, J. F.; Truss, R. W.; Geil, P. H. J Macromol Sci, Phys, 1981, B19, 313.
4. Aharoni, S. M.; Sibilia, J. P. Polym Eng Sci, 1979, 19, 450.
5. Ishihara, N.; Kuramoto, N.; Uoi, M. Macromol, 1988, 21, 3356.
6. Koch-Preuss, U. Kunststoffe Plast Eur, 1998, 17.
7. Guerra, G.; Vitagliano, V. M.; De Rosa, C.; Petraccone, V.; Corradini, P. Macromol, 1990, 23, 1539.
8. Chatani, Y.; Fujii, Y.; Shimane, Y.; Ijitsu, T. Polym Prepr Jpn (Eng Ed), 1988, 37, E428.
9. Immirzi, A.; De Candia, F.; Iannelli, P.; Vittoria, V.; Zambelli, A. Makromol Chem Rapid Comm, 1988, 9, 761.
10. Kellar, E. J. C.; Galiotis, C.; Andrews, E. H. Macromol 1996, 29, 3515.
11. Po', R.; Cardi, N.; Abis, L. Polymer 1998, 39, 959.
12. Sun, Z.; Morgan, R. J.; Lewis, D. N. Polymer, 1992, 33, 660.
13. Reynolds, N. M.; Stidham, H. D.; Hsu, S. L. Macromol 1991, 24, 3662.
14. Pasztor, Jr., A. J.; Landes, B. G.; Karjala, P. J. Thermochim Acta 1991, 177, 187.
15. Manfredi, C.; De Rosa, C.; Guerra, G;. Rapacciuolo, M.; Auriemma, F.; Corradini, P. Macromol Chem Phys 1995, 196, 2795.
16. Greis, O.; Xu, Y.; Asano, T.; Peterman, J. Polymer 1989, 30, 590.